# Controlled Molecular Alignment in Phthalocyanine Thin Films on Stepped Sapphire Surfaces**

By *J. Oriol Ossó*, *Frank Schreiber*,* *Volker Kruppa*, *Helmut Dosch*, *Miquel Garriga*, *M. Isabel Alonso*, and *Fernando Cerdeira*

We report a detailed study of the growth and structure of thin films of copper hexadecafluorophthalocyanine ($F_{16}$CuPc) on sapphire. These films show very good out-of-plane order and have X-ray rocking widths of around 0.02°. If prepared under suitable conditions on *A*-plane sapphire substrates, the molecules align without significant azimuthal dispersion. Growth on MgO (001) and oxidized silicon wafers resulted in a comparable out-of-plane structure, but showed no azimuthal order. We find that the azimuthal alignment on sapphire is induced by the step edges along the *c*-axis of the sapphire, which serve as templates for the growth. For growth at different substrate temperatures, we find a monotonic change of the molecular out-of-plane tilt angle, as obtained from Raman scattering, which is accompanied by a change of the out-of-plane lattice parameter.

## 1. Introduction

Due to their attractive electronic and optical properties, organic semiconductors are presently receiving a lot of attention. Although several applications have already been demonstrated, it has also become clear that the performance of a device depends crucially on the structural definition of these systems. For the preparation of thin films, organic molecular beam deposition (OMBD) holds the promise for optimum control of the structure.[1–4] Despite much effort in recent years, there are still several challenges to face, some of which are inherently related to the nature of these relatively large molecules.[1,2] First of all, the unit cells of these materials are large compared to those of typical inorganic substrates, and they exhibit, in many cases, a very low symmetry. This frequently leads to multiple rotational and translational domains, which hamper the formation of single-domain films. Secondly, the chemical nature of the substrate is crucial. Strongly interacting substrates usually limit the surface mobility of the molecules during film formation, thus leading to a high density of grains, whereas weakly interacting substrates, in many cases, lead to the islanding of the films, i.e., morphologies characteristic of dewetting. Only certain systems and crystallographic orientations appear suitable for the combination of a smooth and non-dewetting film morphology and good crystallinity. Even if this is accomplished, in-plane epitaxial alignment remains a challenge, in particular due to the formation of multiple symmetry-equivalent domains.[1,3,5,6]

In this paper, we report the results of a detailed study of the growth and structure of thin films of copper hexadecafluorophthalocyanine ($F_{16}$CuPc) on *A*-plane sapphire[7] with a small but finite miscut (see Fig. 1). The associated regular surface steps served as templates for the growth of crystalline $F_{16}$CuPc films, by favoring only one azimuthal orientation. The concept of stepped substrates[8] has been used frequently for monolayer adsorbates;[9] however, here we demonstrate its use for comparatively thick films (5 to 50 ML) of relatively large molecules. $F_{16}$CuPc was chosen since it is considered a good candidate as an n-type conducting organic material.[10] Being a blue dye, it is also interesting for optoelectronic applications.[11,12] Moreover, phthalocyanines exhibit a certain degree of "specific tunability" due to the central metal ion, which can be changed over a broad range.[12] The films were investigated for different thicknesses and preparation temperatures. We found that films grown under suitable conditions exhibited a smooth morphology and no multiple azimuthal domains.

## 2. Results

We will discuss two sets of films: i) films of fixed thickness (20 nm) and various growth temperatures; and ii) films of various thickness grown at a fixed temperature ($T_g$ = 230 °C). A study of the film properties for $T_g$ in the range between –150 and 250 °C revealed that order increases with increasing $T_g$. To analyze this ordered structure, films with thicknesses $d$ = 5, 12, 20, 25, 30, and 45 nm were grown at $T_g$ = 230 °C. In order to obtain a comprehensive picture, several complementary techniques, which are sensitive to different aspects of the ordering, were employed.

[*] Dr. F. Schreiber,[+] J. O. Ossó, Dr. V. Kruppa, Prof. H. Dosch
Max-Planck-Institut für Metallforschung
Heisenbergstr. 1, D-70569 Stuttgart (Germany)
J. O. Ossó, Dr. M. Garriga, Dr. M. I. Alonso, Dr. F. Cerdeira
Institut de Ciència de Materials de Barcelona, CSIC
E-08193 Bellaterra (Spain)
Dr. F. Schreiber,[+] Prof. H. Dosch
Institut für Theoretische und Angewandte Physik, Universität Stuttgart
D-70550 Stuttgart (Germany)
Dr. F. Cerdeira
Instituto de Fsica "Gleb Wataghin", UNICAMP
13.083-970 Campinas S.P. (Brazil)
[+] Present address: Physical and Theoretical Chemistry Laboratory, University of Oxford, South Parks Road, Oxford OX1 3QZ, UK.
E-mail: frank.schreiber@chem.ox.ac.uk.

[**] The authors acknowledge their pleasant cooperation with B. Krause, A. C. Dürr, S. Sellner, E. Barrena, K. A. Ritley, M. Schlestein, D. Epple, H. Bender, J. Pflaum, N. Karl, and H. Port. They acknowledge financial support from the Max–Planck–Gesellschaft and from the DFG (Schwerpunktprogramm "Organische Feldeffekt-Transistoren"). They are grateful to N. Karl and S. Hirschmann for purifying the materials.

  1616-301X/02/0706-0455 $ 17.50+.50/0 

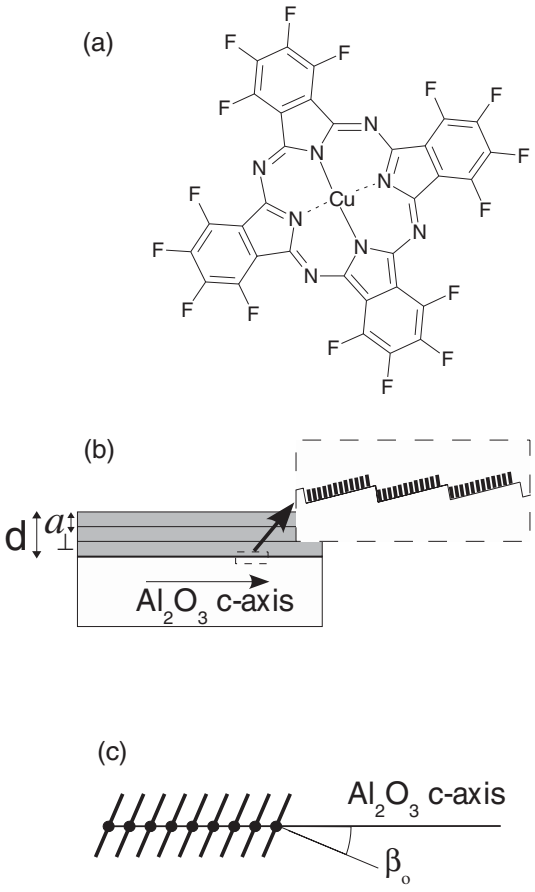


Fig. 1. a) Molecular structure of copper hexadecafluorophthalocyanine ($F_{16}$CuPc). b) Schematic of the film structure (side view), where $d$ is the total film thickness and $a_\perp$ is the out-of-plane lattice spacing. A magnified view of the interface $Al_2O_3$/$F_{16}$CuPc shows the step-induced orientation of the molecules. c) Schematic of the film structure (top view). $\beta_0$ is the angle between the normal to the molecular plane and the $Al_2O_3$ *c*-axis.

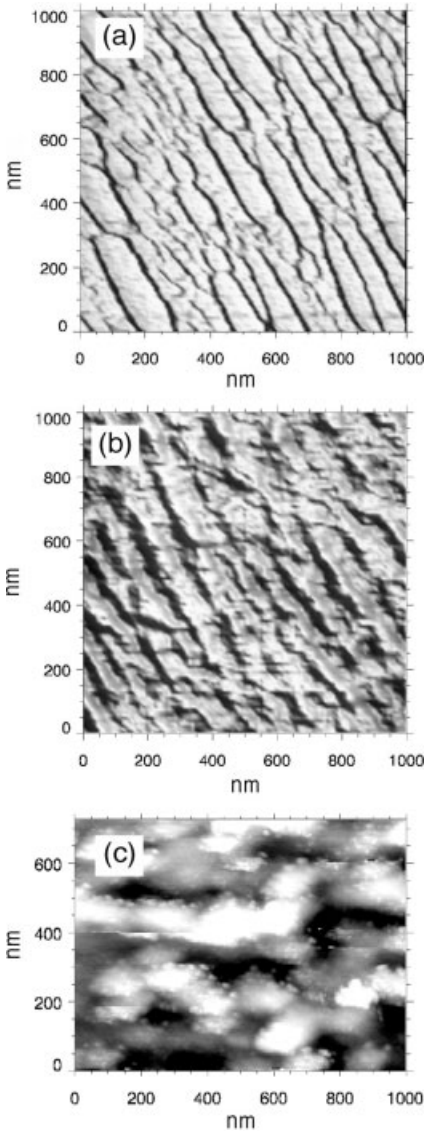


Fig. 2. a) AFM image of an $Al_2O_3$ surface before film growth. Non-contact AFM images of $F_{16}$CuPc films on $Al_2O_3$ grown at b) 230 °C and c) –150 °C.

### 2.1. Atomic Force Microscopy

Atomic force microscopy (AFM) was used to investigate the morphology of the films and the substrates. Figure 2b shows the AFM image of a 12 nm film grown at 230 °C. Parallel stripes with a typical separation of about 100 nm were observed in all the films grown at this temperature. Comparing this image (Fig. 2b) with that of the substrate surface (Fig. 2a), it is easily seen that the film's morphology follows the stepped substrate surface and the terraces are propagated through the $F_{16}$CuPc film. The images were analyzed using local slope histograms (LSH) to quantify the anisotropic morphology of the films. A radial integration (Fig. 3b) of the LSH image for each azimuth in Fig. 3a allowed us to quantify the directionality of the local slope, i.e., it shows the anisotropy of the "waves" building up the surface roughness. The symmetry of the surface morphology of the film from Figure 2b is evident in the LSH shown in Figure 3.

Apart from the substrate-induced steps, the films tend to exhibit a smooth morphology and smaller roughness at higher temperatures, suggesting that the system can be viewed as "wetting", in contrast to, e.g., 3,4,9,10-perylenetetracarboxylic dianhydride (PTCDA) on various substrates.[5,6] However, as the film thickness was increased, a small but monotonic increase in roughness from 0.3 nm, at $d$ = 12 nm, to 1.2 nm at $d$ = 45 nm was found by AFM, which is consistent with the X-ray data. A strong morphology change was observed when the growth temperature was decreased to –150 °C. The stripes described above for films grown at 230 °C were not present for low-temperature films. Instead, as can be seen in Figure 2c, more or less rounded crystallites were observed, forming a rougher surface. Whereas the root mean square (rms) roughness $\sigma$ determined from Figure 2b ($T_g$ = 230 °C) was as low as 0.3 nm, for Figure 2c ($T_g$ = –150 °C) $\sigma$ was 2.8 nm.

### 2.2. X-ray Scattering

X-ray scattering is sensitive to the crystalline order and the interface quality of a film. Measurements along the surface nor-

  1616-301X/02/0706-0456 $ 17.50+.50/0 

ADVANCED FUNCTIONAL MATERIALS



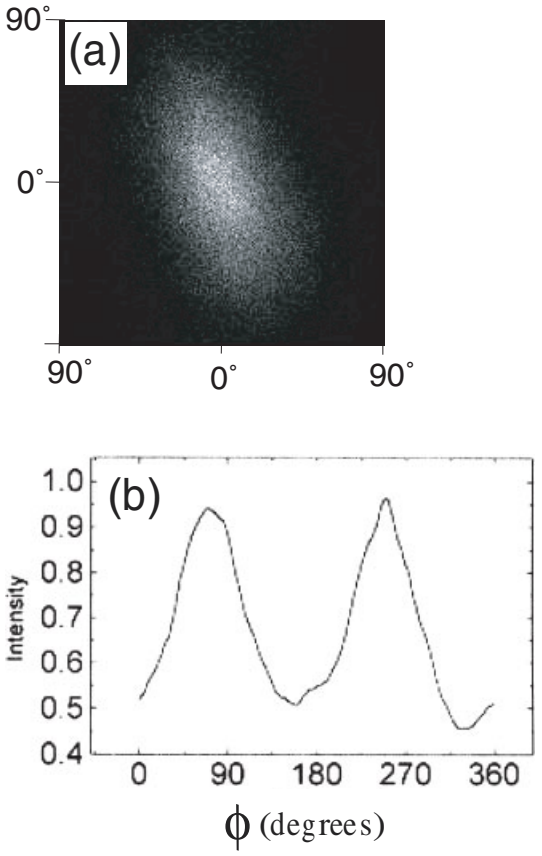


Fig. 3. a) Local slope histogram (LSH) of Figure 2b. This method evaluates the direction of the surface normal, $\hat{n}$. Defining a coordinate system with the $x$ and $y$ axes in the image plane, and $\alpha_x$ ($\alpha_y$) as the angle(s) between the projection of the vector $\hat{n}$ on the $x$–$z$($y$–$z$) plane and the $z$-axis, then the orientation of $\hat{n}$ is defined by $\alpha_x$ and $\alpha_y$, and $\hat{n}$ can be correlated with a point in the plane $\alpha_x - \alpha_y$, where $\alpha_x$, $\alpha_y \in [-90°, 90°]$. Following this procedure at each point of the AFM image, the LSH was obtained, where the intensity at a given point ($\alpha_x$, $\alpha_y$) is proportional to the number of projections of $\hat{n}$ with these values. b) Radial integration of the LSH.

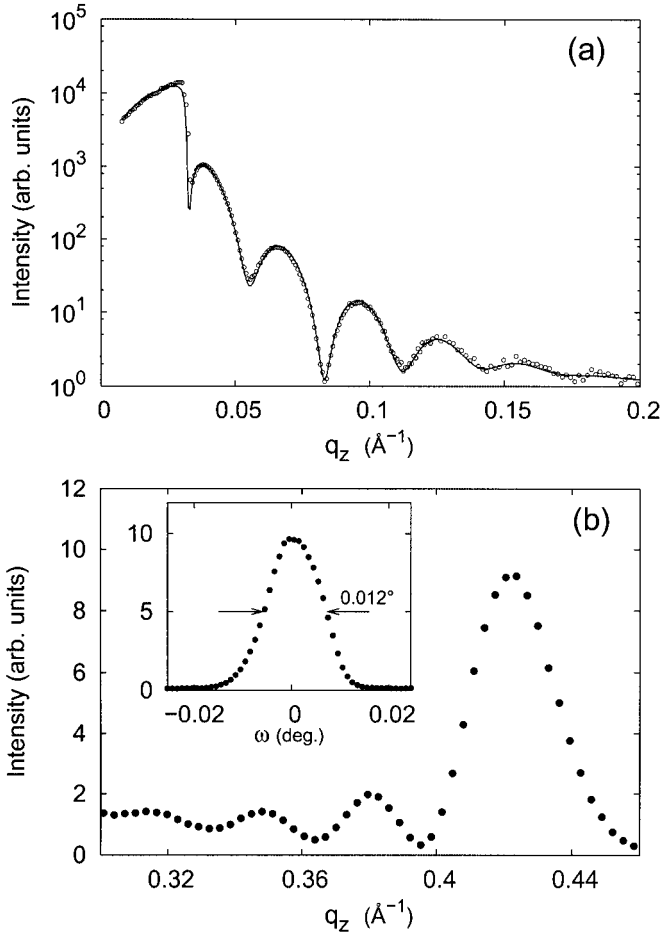


Fig. 4. a) Reflectivity scan on a 20 nm film grown at 230 °C on $SiO_2$, including a fit (solid line) according to the Parratt formalism. b) First order Bragg reflection at $q_z = 0.424$ Å$^{-1}$. The inset shows a rocking scan on the Bragg reflection.

mal (Fig. 4) revealed an out-of-plane lattice spacing $a_\perp$ around 15 Å. This suggests an arrangement with the molecules "standing" essentially upright, as shown schematically in Figure 1b. The exact value of $a_\perp$ depended on the growth conditions. This orientation is interesting for applications, since it supports in-plane charge transport, due to the overlap of the π-orbitals in the film plane. Figure 4 shows a typical scan in the reflectivity regime, with well-defined Kiessig interferences and the first-order Bragg reflection with accompanying Laue oscillations. The inset shows a rocking scan with a width as low as 0.012°.

Upon increasing $T_g$, a monotonic increase of the lattice constant, $a_\perp$, from 14.6 Å for samples grown at room temperature to 15.3 Å for samples grown at 250 °C was found. This is consistent with the Raman results, as explained below. For films grown at –150 °C, a broadened Bragg reflection revealed a lower out-of-plane coherence length, and a larger mosaicity (0.1°). The Kiessig interferences and the Laue oscillations were more pronounced for films grown at elevated temperature, implying better defined interfaces and crystalline coherence. Thus, from both AFM and X-ray scattering results, significant structural differences were found for low $T_g$ compared to high $T_g$.

Grazing incidence X-ray diffraction (GIXRD) measurements (Fig. 5) using $\lambda = 0.71$ Å revealed an in-plane Bragg reflection at $2\Theta = 12.87°$ for samples grown at $T_g = 230$ °C, which

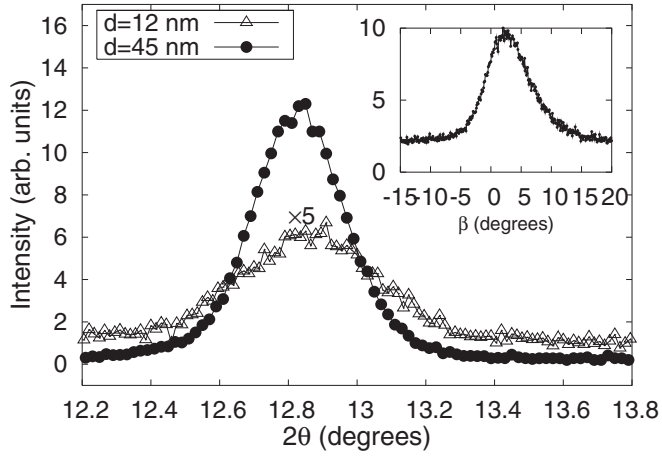


Fig. 5. In-plane Bragg reflection at $2\Theta = 12.87°$ ($\lambda = 0.71$ Å) for films grown at $T_g = 230$ °C, on $Al_2O_3$ with thicknesses of 12 and 45 nm. The scan for the 12 nm film has been multiplied by a factor of 5 for clarity. The accuracy in $2\Theta$ of this scan was 0.11°. The inset shows the rocking scan of the 12 nm film, where $\beta$ is the azimuthal orientation relative to the $Al_2O_3$ $c$-axis.

  1616-301X/02/0706-0457 $ 17.50+.50/0 

corresponds to a lattice spacing of $a_{\|}$ = 3.2 Å. The radial width of the peak was found to be $\Delta\Theta = 0.27°$, which corresponds to coherent domains of at least 15 nm, without a strong dependence on film thickness. The inset of Figure 5 shows an azimuthal scan across the in-plane Bragg reflection, showing the preferred orientation of the structure. The width, i.e., the degree of azimuthal disorder, was found to decrease with increasing film thickness, as shown in Figure 6a, from 10° for $d$ = 12 nm down to 4° for $d$ = 45 nm. Obviously, once a certain degree of order has been induced by the substrate, for subsequent growth the film prefers to adopt a well-defined crystalline orientation.

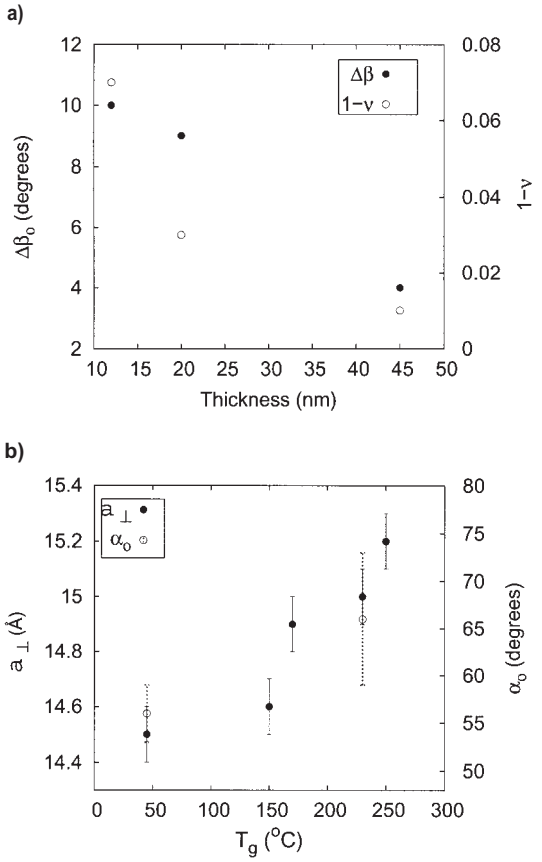


Fig. 6. a) Full width at half maximum ($\Delta\beta_0$) of the 12.87° reflection obtained from X-ray scattering, and 1–$\nu$, as a function of film thickness. b) Values of the out-of-plane lattice constant $a_\perp$ obtained from X-ray scattering, together with the values of $\alpha_0$ derived from Raman scattering, for a 20 nm film.

The (0001) reflection from the $Al_2O_3$ substrate was used to determine the angle $\beta_0$ between the direction of the lattice planes of the film and the $c$-axis (see Fig. 1c). From GIXRD, $\beta_0$ values of around 2° were found. Similar values were obtained from Raman and ellipsometry data.[13] Note that GIXRD measures the angle between the *lattice* planes and the $c$-axis, rather than the angle between the *molecular* plane and the $c$-axis, as Raman scattering does for the modes under consideration. For films on $Si/SiO_2$, the same in-plane Bragg reflection around 12.87° was found, but on this amorphous flat surface the films are, of course, azimuthally isotropic.

### 2.3. Raman Scattering

Raman spectra of the $F_{16}CuPc$ films show several lines between 150 and 1600 cm$^{-1}$. The observed line positions were essentially independent of the substrate. The line intensities for the films grown on $Si/SiO_2$ and MgO substrates were similar and independent of the azimuthal angle, $\beta$, but, for samples grown on sapphire, the scattered intensities displayed a characteristic dependence on $\beta$, which was used to analyze the molecules' orientation. For the quantitative analysis appropriate expressions[13] for the angular variation of the intensity were derived from the selection rules corresponding to either the tetragonal point group of the $F_{16}CuPc$ molecules, or to the monoclinic group in which metal-phthalocyanines typically crystallize. The azimuthal dependence agrees with the expected variation of the scattered intensity for molecular modes with $A_{1g}$ symmetry:

$$I(\beta) = A^2(\sin^2\alpha_0\cos^2(\beta-\beta_0) + \cos^2\alpha_0)^2 + C \quad (1)$$

where $\alpha_0$ and $\beta_0$ are defined in Figure 1. $\alpha_0$ is not defined in Figure 1. $A$ and $C$, respectively, are parameters for the $A_{1g}$ mode strength and the background (from the disordered part of the sample). In Figure 7, the azimuthal dependence of the

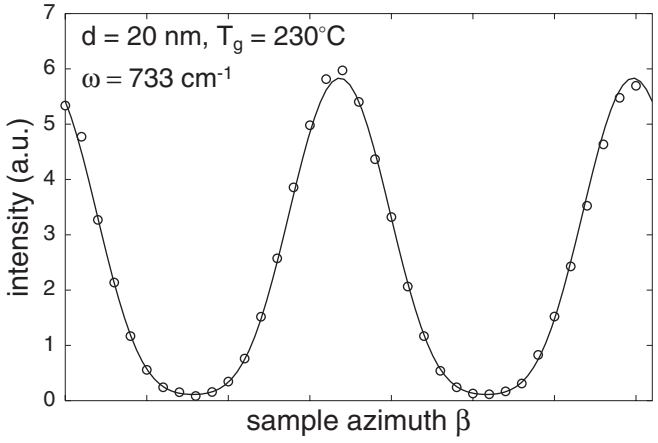


Fig. 7. The measured dependence of the backscattered intensity on the sample azimuth for the 733 cm$^{-1}$ Raman line in direct polarization. The solid line is a fit of the experimental data (circles) to Equation 1.

733 cm$^{-1}$ mode is shown. A similar dependence was observed for practically all the Raman lines. $\alpha_0$ ranged between 56 and 66°. In Figure 6b, the $\alpha_0$ values for the 20 nm films are shown as a function of $T_g$. To quantify the observed structural order, we defined the parameter $\nu = A^2/(A^2 + C)$. Values of $\nu$ ranged from 0.93 to 0.99, and increased with increasing growth temperature. As shown in Figure 6a, the thickness dependence of the disorder (1–$\nu$) from the Raman data correlates with the azimuthal disorder obtained from GIXRD, i.e., they both decrease with increasing $d$.

  1616-301X/02/0706-0458 $ 17.50+.50/0 

ADVANCED FUNCTIONAL MATERIALS



### 2.4. Spectroscopic Ellipsometry

The substrate-induced controlled alignment of the $F_{16}CuPc$ molecules in the films should give rise to pronounced anisotropies of the collective optical properties. This was indeed reflected in the spectroscopic ellipsometry data, as shown in Figure 8. Anisotropic behavior was found for all films grown on *A*-plane sapphire at high temperature. These films behaved as optically biaxial media with two principal axes in the sample

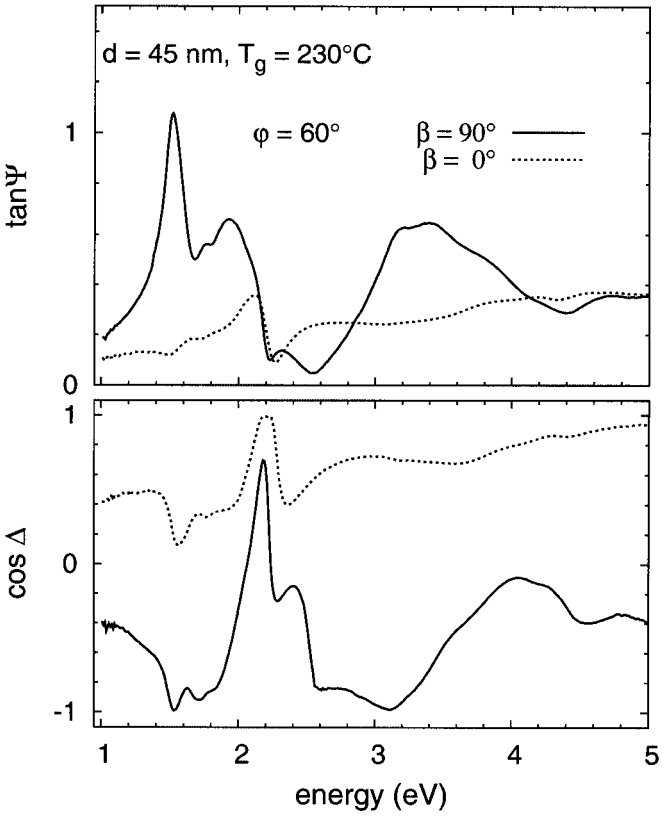


Fig. 8. Dependence of the ellipsometric parameters on the sample azimuth $\beta$, measured at an angle of incidence of 60°. The spectra polarized along the step edges (solid lines) exhibit the most pronounced features, especially visible in tan$\Psi$, associated with electronic transitions within the molecular planes.

surface, essentially coinciding with the substrate *c*-axis direction and the axis perpendicular to it. The main spectral features were polarized in the latter direction, in agreement with molecules "standing-up" essentially parallel to the step edges. Generally, spectra taken at four different sample azimuths along the principal axes are sufficient to demonstrate the anisotropy and to extract the in-plane components of the optical function tensors.[13] No dependence on sample azimuth was found for samples grown on MgO and $SiO_2$ substrates.

## 3. Summary and Conclusions

We have studied thin films of $F_{16}CuPc$ grown on stepped $Al_2O_3$ surfaces. If prepared under suitable conditions, a strong in-plane anisotropy was obtained, as observed by the techniques used (AFM, X-ray scattering, spectroscopic ellipsometry, and Raman scattering). This anisotropy appears to be induced by the specific stepped morphology of the $Al_2O_3$ surface. The step edges act as a template for the first few monolayers, aligning the molecules in a preferred orientation. This behavior has been observed for other systems, mostly using smaller molecules[9,14,15] or monolayers.[16] The fact that the anisotropy increases with film thickness suggests that successive layers continue with the pattern defined by the earlier layers, suppressing the formation of azimuthal domains. For the present system, the step-induced alignment was only found in high-temperature films, presumably since only for these was the diffusion of the ad-molecules on the terraces sufficiently large. When the growth temperature was decreased, a higher azimuthal disorder and a rougher morphology were obtained, accompanied by a monotonic decrease of the out-of-plane lattice spacing and tilt angle.

It is well-known that electronic transport properties, particularly the charge carrier mobility, depend strongly on the degree of structural order.[17,18] The charge transport in $F_{16}CuPc$ polycrystalline thin film devices has been shown to be controlled by grain boundary effects.[19] Generally, many organic thin film systems encounter complications due to multiple symmetry-equivalent domains, which result in grain boundaries. These problems may be overcome by suitably stepped substrate surfaces, as demonstrated in the present work. We expect that this concept will prove to be fruitful for efficient in-plane charge carrier transport and a number of applications based on it.

## 4. Experimental

The films were grown in an ultra high vacuum (UHV) chamber with a base pressure of $10^{-10}$ mbar. The $F_{16}CuPc$ powder was purchased from Aldrich Chemical Co. and purified twice by gradient sublimation prior to evaporation from a custom-built Knudsen cell. During deposition, the cell temperature was kept above 400 °C and the pressure in the chamber typically rose to ~$3 \times 10^{-9}$ mbar. The film's thickness and deposition rate were monitored by a quartz-crystal monitor (QCM) placed close to the substrate. Films of different thicknesses were prepared over a temperature range from –150 to 250 °C, with an impingement rate of about 4 Å/min. All films were grown simultaneously on three different substrates, namely on $Al_2O_3$ (1120) (*A*-plane), and, for comparison, on Si (100) with native oxide, and on MgO (100). Prior to film growth, the $Al_2O_3$ (1120) substrates were annealed to 1500 °C for 48 h, in air. As a consequence of the surface miscut, a step pattern was induced. As shown in Figure 2a, the surface after annealing exhibited terraces ~130 nm wide and ~1.8 nm in step height. The miscut of the substrate series used was 0.57, as determined by X-ray diffraction. Before growth, the substrates were ultrasonically cleaned with organic solvents (acetone, ethanol) and heated under UHV to 700 °C, typically for 10 h.

Atomic force microscopy (AFM) was performed in the non-contact mode (NC–AFM) under UHV in a commercial system (Omicron), using single-crystalline Si cantilevers with frequencies from 269 to 311 kHz. The tip radii were typically around 10 nm. The NC–AFM images shown are unfiltered, except for the subtraction of a constant background. The X-ray measurements were performed using in-house X-ray stations in different scattering geometries using Cu K$\alpha$ ($\lambda$ = 1.79 Å) and Mo K$\alpha$ ($\lambda$ = 0.71 Å). Specular reflectivity was used to characterize the electron density profile, $\rho_e(z)$, along the surface normal, i.e., to measure film thickness and density, the interfacial roughness, density, out-of-plane lattice spacing, and crystalline coherence length. The reflectivity data were analyzed using the Parratt formalism, which takes into account multiple scattering effects [20]. GIXRD [21] was used to determine the in-plane structure and degree of epitaxial alignment of the film.

Raman scattering measurements were carried out using the 514.5 nm line of an Argon-ion laser focused with a microscope objective (×50) to a spot size of about 2 μm in diameter, with an incident power density of ~$1.5 \times 10^4$ W/cm$^2$. The backscattered light was collected with the microscope and analyzed with a triple

  1616-301X/02/0706-0459 $ 17.50+.50/0 

ADVANCED FUNCTIONAL MATERIALS



spectrometer (Jobin Yvon T-4000 XY) and a charge coupled device detector cooled with liquid nitrogen. Polarization dependent measurements were done in the 150 to 1600 $cm^{-1}$ spectral range, with a resolution of ~2 $cm^{-1}$. For a quantitative analysis of the angular dependence of the Raman scattered intensity, samples were mounted on a goniometer and rotated around the surface normal, i.e., the direction of the incident light.

Spectroscopic ellipsometry measurements were performed with a rotating analyzer ellipsometer using a 75 W high-pressure Xe lamp as the light source and a 750 mm equivalent focal length double prism/grating spectrometer. As detectors, we used a multialkali photomultiplier for the UV-vis range, and a GaInAs photodiode below 1.4 eV, which covered the spectral range from 0.7 to 5.1 eV, with a resolution of around 1 meV. Data were taken at an angle of incidence of 60 or 70°. To assess the in-plane film anisotropy, the sample holder was mounted on a goniometer and spectra were taken at different sample azimuths.

Received: February 5, 2002
Final version: March 18, 2002

[1] S. R. Forrest, *Chem. Rev.* **1997**, *97*, 1793.
[2] E. Umbach, M. Sokolowski, R. Fink, *Appl. Phys. A* **1996**, *63*, 565.
[3] W. Kowalsky, T. Benstem, A. Böhler, S. Dirr, H.-H. Johannes, D. Metzdorf, H. Neuner, J. Schöbel, P. Urbach, *Phys. Chem. Chem. Phys.* **1999**, *1*, 1719.
[4] D. E. Hooks, T. Fritz, M. D. Ward, *Adv. Mater.* **2001** *13*, 227.
[5] B. Krause, A. C. Dürr, K. A. Ritley, F. Schreiber, H. Dosch, D. Smilgies, *Appl. Surf. Sci.* **2001**, *175–176*, 332.
[6] P. Fenter, F. Schreiber, L. Zhou, P. Eisenberger, S. R. Forrest, *Phys. Rev. B* **1997**, *56*, 3046.
[7] T. Becker, A. Birkner, G. Witte, C. Wöll, *Phys. Rev. B* **2002**, *65*, 115 401.
[8] P. W. Carter, M. D. Ward, *J. Am. Chem. Soc.* **1993**, *115*, 11 521; this reference refers to organic–on–organic growth.
[9] S. Lukas, S. Vollmer, G. Witte, C. Wöll, *J. Chem. Phys.* **2001**, *114*, 10 123
[10] Z. Bao, A. J. Lovinger, J. Brown, *J. Am. Chem. Soc.* **1998**, *120*, 207.
[11] J. A. Rogers, Z. Bao, A. Dodabalapur, A. Makhija, *IEEE Electron Device Lett.* **2000**, *21*, 100.
[12] C. C. Leznoff, A. B. P. Lever, *Phthalocyanines: Properties and Applications*, VCH, New York **1989**.
[13] M. Garriga, F. Cerdeira, M. I. Alonso, unpublished results.
[14] T. Hayashi, T. Maruno, A. Yamashita, S. Fölsch, H. Kanbara, H. Konami, M. Hatano, *Jpn. J. Appl. Phys.* **1995**, *34*, 3884.
[15] T. Maruno, A. Yamashita, T. Hayashi, H. Konami, M. Hatano, Y. Shiratori, K. Ohhira, *Jpn. J. Appl. Phys.* **1993**, *32*, L628.
[16] I. Chizhov, G. Scoles, A. Kahn, *Langmuir* **2000**, *16*, 4358.
[17] G. Horowitz, M. E. Hajlaoui, *Synth. Met.* **2001**, *122*, 185.
[18] N. Karl, J. Marktanner, *Mol. Cryst. Liq. Cryst.* **1998**, *315*, 163.
[19] J. H. Schön, C. Kloc, Z. Bao, B. Batlogg, *Adv. Mater*, **2000**, *12*, 1539.
[20] M. Tolan, *X-Ray Scattering from Soft-Matter Thin Films*, Springer Tracts in Modern Physics, Vol. 148, Springer, Heidelberg **1999**.
[21] H. Dosch, *Critical Phenomena at Surfaces and Interfaces*, Springer Tracts in Modern Physics, Vol. 126, Springer, Heidelberg **1992**.

  1616-301X/02/0706-0460 $ 17.50+.50/0 